

**Percolation of heteronuclear dimers irreversibly deposited on square lattices**

M. C. Gimenez\*

*Facultad de Matemática, Astronomía Física y Computación, U.N.C., Córdoba, IFEG-CONICET, Córdoba 5000, Argentina*

A. J. Ramirez-Pastor

*Departamento de Física, Instituto de Física Aplicada (INFAP), Universidad Nacional de San Luis-CONICET, Ejército de Los Andes 950, D5700HHW San Luis, Argentina*

(Received 9 June 2016; published 26 September 2016)

The percolation problem of irreversibly deposited heteronuclear dimers on square lattices is studied. A dimer is composed of two segments, and it occupies two adjacent adsorption sites. Each segment can be either a conductive segment (segment type *A*) or a nonconductive segment (segment type *B*). Three types of dimers are considered: *AA*, *BB*, and *AB*. The connectivity analysis is carried out by accounting only for the conductive segments (segments type *A*). The model offers a simplified representation of the problem of percolation of defective (nonideal) particles, where the presence of defects in the system is simulated by introducing a mixture of conductive and nonconductive segments. Different cases were investigated, according to the sequence of deposition of the particles, the types of dimers involved in the process, and the degree of alignment of the deposited objects. By means of numerical simulations and finite-size scaling analysis, the complete phase diagram separating a percolating from a nonpercolating region was determined for each case. Finally, the consistency of our results was examined by comparing with previous data in the literature for linear *k*-mers (particles occupying *k* adjacent sites) with defects.

DOI: [10.1103/PhysRevE.94.032129](https://doi.org/10.1103/PhysRevE.94.032129)**I. INTRODUCTION**

The study of systems of large particles, particularly dimers, is one of the central problems in statistical mechanics, and it has attracted the attention of researchers for several decades [1–28]. In this framework, many authors have focused their investigations on monolayer films of dimers formed on uniform surfaces, and especially on the percolation properties of these systems [19–28].

Percolation is one of the most studied discrete models in statistical physics [29–36], in which sites or bonds of a lattice are randomly occupied with a probability  $p$  or empty (nonoccupied) with a probability  $1 - p$ . Nearest-neighbor occupied sites (bonds) form structures called clusters. The behavior of the lattice depends on the size and shape of the clusters. When the occupation probability exceeds a critical value (called the percolation threshold  $p_c$ ), a macroscopic, spanning, or infinite cluster, occupying a finite fraction of the total number of sites (bonds), emerges. The percolation transition is then a geometrical phase transition where the critical concentration separates a phase of finite clusters ( $p < p_c$ ) from a phase where an infinite cluster is present ( $p > p_c$ ).

More general percolation problems can be formulated by assuming that the element deposited occupies more than one site (bond) on the lattice. In contrast to the statistic for the simple particles, the problem becomes considerably difficult when some sort of correlation exists, and there have been a few studies devoted to the problem of percolation of structured objects. In Ref. [19], a model involving the formation of dimers on the surface was employed to describe the nonlinear dependence of transport properties on composition in mixed-alkali

ionic conductors. Along the same lines, Holloway [20] studied the problem of site percolation on a diamond lattice occupied by a mixture of monatomic and diatomic species. The results allowed us to understand some of the features of the alloys of Ge with group III-V semiconductors. The dimer problem was also addressed by Gao *et al.* [21], who investigated the process of dissociative adsorption of dimers and studied the percolating properties of dissociated monomers as a function of both the concentration of dimers and the dissociation probability. A phase diagram separating a percolating from a nonpercolating region was obtained.

More recently, a generalization of the site-bond percolation problem, in which pairs of nearest-neighbor sites (site dimers) and pairs of nearest-neighbor bonds (bond dimers) are independently occupied, was studied on a square lattice [22]. The complete phase diagram of the system was obtained. Tarasevich and Cherkasova [23] investigated the percolation and jamming properties of dimers on three-dimensional (3D) simple-cubic lattices. Later, percolation and jamming phenomena were studied for anisotropic sequential deposition of dimers on a square lattice [24]. The influence of dimer alignment on electrical conductivity was examined.

The results in Refs. [19–24] were calculated by means of numerical simulations. From a theoretical point of view, the inherent complexity of the system still represents a major difficulty in the development of accurate analytical solutions. One way to overcome these theoretical complications is to develop simplified models. Along these lines, a cluster-exact approximation was recently introduced [25–27]. This theoretical approach, based on the exact calculations on finite cells, allowed us to study the percolation of site dimers [25] and bond dimers [27] on square lattices, and the site-bond percolation problem for triangular lattices [26].

In all of the papers mentioned above [19–28], the study was restricted to (i) homonuclear dimers and (ii) homogeneous

---

\*Author to whom all correspondence should be addressed: [cgimenez@famaf.unc.edu.ar](mailto:cgimenez@famaf.unc.edu.ar)

surfaces. In the case of point (ii), the effect of surface heterogeneity on the percolation properties of irreversibly deposited dimers was analyzed in a recent paper from our group [28]. In Ref. [28], the heterogeneous substrate was represented by two kinds of sites forming square patches of  $l \times l$  sites, which can be arranged either in a deterministic chessboard structure or in a random way. Thus, the system was characterized by the distribution (ordered or random) of the patches, the patch size  $l$ , and the probability of occupying each patch  $\theta_1$  and  $\theta_2$ . By means of numerical simulations and finite-size scaling analysis, a complete  $(\theta_1 - \theta_2 - l)$  phase diagram separating a percolating and a nonpercolating region was determined.

With respect to point (i), there is a lack of systematic studies addressing the percolation problem of heteronuclear dimers. The objective of this paper is to provide a thorough study in this direction. For this purpose, extensive numerical simulations have been performed to study the percolation of dimers composed of segments  $A$  and  $B$ . Three types of particles were considered:  $AA$ ,  $BB$ , and  $AB$ . The model offers a simplified representation of the problem of percolation of defective (non-ideal) particles, where the presence of defects in the system is simulated by introducing a mixture of conductive or ideal segments ( $A$ ) and nonconductive or imperfect segments ( $B$ ). The results obtained are discussed and compared with data from Ref. [23], where the effect of defects on the percolation of linear  $k$ -mers (particles occupying  $k$  adjacent sites) was studied.

This paper is organized as follows: The model and the simulation technique used to obtain the desired quantities for describing the percolation phase transition are described in Sec. II. Results are presented and discussed in Sec. III. Finally, some conclusions are drawn in Sec. IV.

## II. MODEL AND CALCULATION METHOD

The substrate is represented by a two-dimensional square lattice of  $M = L \times L$  sites with periodic boundary conditions. A dimer is composed of two segments, and it occupies two adjacent adsorption sites. Thus, a lattice site is occupied by one segment or it is empty. Each segment can be either a conductive segment (segment type  $A$ ) or a nonconductive segment (segment type  $B$ ). Three types of dimers have been considered:  $AA$ ,  $BB$ , and  $AB$ , and the connectivity analysis is carried out by accounting only for the conductive segments (type  $A$ ).

To rationalize our study, three different cases have been considered, according to (i) the sequence of deposition of the particles and (ii) the types of dimers involved in the process:

*Model I.* Starting from an initially empty lattice,  $AA$  dimers are deposited until a coverage  $\theta_{AA}$  is reached. In a second stage, a fraction  $\theta_{AB}$  of  $AB$  dimers is deposited on the lattice. To facilitate the presentation in this section, the coverage reached in the first stage will be denoted by  $\theta_1$ , and the coverage reached in the second stage will be denoted by  $\theta_2$ . In this case,  $\theta_1 = \theta_{AA}$  and  $\theta_2 = \theta_{AB}$ .

*Model II.* Starting from an initially empty lattice,  $AB$  dimers are deposited until a coverage  $\theta_1 = \theta_{AB}$  is reached. In a second stage, a fraction  $\theta_2 = \theta_{AA}$  of  $AA$  dimers is deposited on the lattice.

*Model III.* Starting from an initially empty lattice,  $BB$  dimers are deposited until a coverage  $\theta_1 = \theta_{BB}$  is reached. In

a second stage, a fraction  $\theta_2 = \theta_{AA}$  of  $AA$  dimers is deposited on the lattice.

The other possible combinations were not taken into account for the following reasons: In the case of  $\theta_1 = \theta_{BB}$  ( $\theta_{AB}$ ) and  $\theta_2 = \theta_{AB}$  ( $\theta_{BB}$ ), the fraction of conductive segments on the lattice is small, and the system does not percolate. In fact, even for the limiting case of  $\theta_{AB} \approx 0.907$  [37] (and  $\theta_{BB} = 0$ ), the coverage of percolating particles (type  $A$ ) is approximately  $0.907/2 = 0.454$ , while the percolation threshold is around  $0.59$  [34]. On the other hand, the combination  $\theta_1 = \theta_{AA}$  and  $\theta_2 = \theta_{BB}$  is trivial: if  $AA$  dimers were deposited in the first stage, the percolation results would coincide with the standard problem of dimers on square lattices [38,39]. The later deposition of type  $BB$  dimers does not have any influence in the percolation process.

In addition, for each model (I, II, and III), two different cases were investigated, according to the degree of alignment of the deposited objects:

*Isotropic case.* The dimers are deposited isotropically on the lattice (the probability of deposition along the  $x$  axis equals the probability of deposition along the  $y$  axis).

*Nematic case.* The dimers are deposited along one of the directions of the lattice (for instance, along the  $x$  axis), forming a nematic phase.

In the filling process, the dimers are deposited randomly, sequentially, and irreversibly on the lattice. The procedure is as follows:

(i) One lattice site  $i$  is chosen at random.

(ii) If the site  $i$  is empty, then one of the  $z$  nearest neighbors of  $i$  is chosen randomly.  $z = 4$  ( $z = 2$ ) for the isotropic (nematic) case.

(iii) If both sites are unoccupied, a dimer is deposited on those two sites.

(iv) Steps (i)–(iii) are repeated until the desired concentrations  $(\theta_1, \theta_2)$  are reached or until jamming conditions. Due to the blocking of the lattice by the already randomly deposited dimers, the limiting or jamming coverage,  $\theta_j \equiv \theta(t = \infty)$ , is less than that corresponding to the close packing ( $\theta_j < 1$ ). Note that  $\theta(t)$  represents the fraction of lattice sites covered at time  $t$  by the deposited objects. Consequently, the total lattice coverage  $(\theta_1 + \theta_2)$  ranges from 0 to  $\theta_j$ . An extensive overview of this field can be found in the excellent work by Evans in Ref. [6] (and references therein).

The central idea of the percolation theory is based on finding the minimum coverage degree for which at least a cluster (a group of occupied sites in such a way that each one has at least one occupied nearest-neighbor site) extends from one side to the opposite one of the system. This particular value of the coverage degree is called the *critical concentration* or *percolation threshold*, and it determines a phase transition in the system. In the present model, given  $\theta_1$ , we look for the value of  $\theta_2$  for which percolation occurs, and that value will be our percolation threshold  $\theta_2^c$ .

As the scaling theory predicts [40], the larger the system size being studied, the more accurate are the values of the threshold obtained therefrom. Thus, the finite-size scaling theory gives us the basis to achieve the percolation threshold and the critical exponents of a system with reasonable accuracy. For this purpose, the probability  $R = R_L^U(\theta_1, \theta_2)$  that a lattice composed of  $L \times L$  sites percolates at concentrations  $\theta_1$  and

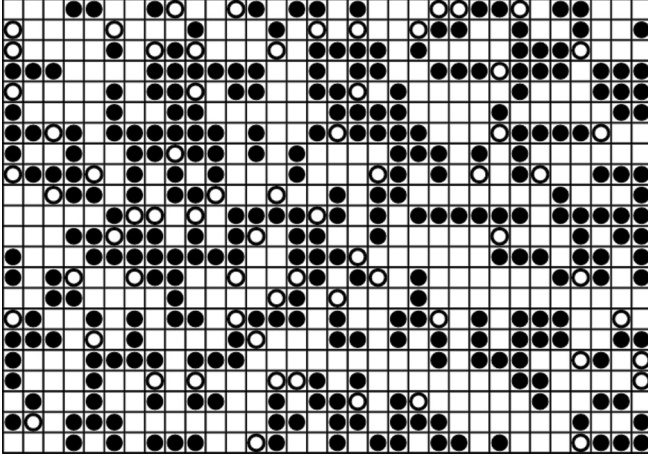


FIG. 1. Snapshot of a typical configuration of dimers deposited on a homogeneous square surface for model II and the isotropic case. The figure shows only a fraction of the whole lattice. Solid circles correspond to  $A$  segments (conductive segments), while open circles represent  $B$  segments (nonconductive segments). In the figure,  $\theta_1 = \theta_{AB} = 0.2$  and  $\theta_2 = \theta_{AA} = 0.3$ .

$\theta_2$  can be defined [34,41,42].  $R_L^U(\theta_1, \theta_2)$  is the probability of finding either a rightward *or* a downward percolating cluster.

In the simulations, each run consists of the following steps: (a) construction of the lattice for the desired fractions ( $\theta_1, \theta_2$ ), according to the scheme mentioned before, and (b) cluster analysis by using the Hoshen and Kopelman algorithm [43].  $n$  runs of two such steps are carried out to obtain the number of runs  $m^U$  for which a percolating cluster is found. Then,  $R_L^U(\theta_1, \theta_2) = m^U/n$  is defined, and the procedure is repeated for a fixed value of  $\theta_1$  and different values of  $\theta_2$ . A set of  $n = 10000$  independent samples is numerically prepared for each model and each pair ( $\theta_1, \theta_2$ ).

The standard theory of finite-size scaling allows us to estimate the percolation threshold from simulation data [34,41,42,44]. The method used here is from the extrapolation of the positions  $\theta_2^c(L)$  of the maxima of the slopes of  $R_L^U(\theta_1, \theta_2)$ . For each size,  $dR_L^U(\theta_1, \theta_2)/d\theta_2$  is calculated and fitted by a Gaussian function. The corresponding value of  $\theta_2^c(L)$  is obtained from the central point of the Gaussian function. The following relationship is expected in order to obtain the extrapolated  $\theta_2^c(\infty)$  value:

$$\theta_2^c(L) = \theta_2^c(\infty) + CL^{-\frac{1}{\nu}} \quad (\text{fixed } \theta_1), \quad (1)$$

where  $C$  is a nonuniversal constant, and the critical exponent  $\nu$  is expected to be equal to  $\nu = 4/3$ , as in the case of standard random percolation [34,38,39,41,42,44].

### III. RESULTS AND DISCUSSION

Figures 1 and 2 show frames corresponding to a portion of the surface covered by dimers deposited according to model II. Solid circles denote  $A$  segments (conductive segments), while open circles represent  $B$  segments (nonconductive segments). The parameters in the figures are as follows: isotropic case with  $\theta_1 = \theta_{AB} = 0.2$  and  $\theta_2 = \theta_{AA} = 0.3$ , Fig. 1; and nematic case with  $\theta_1 = \theta_{AB} = 0.2$  and  $\theta_2 = \theta_{AA} = 0.4$ , Fig. 2.

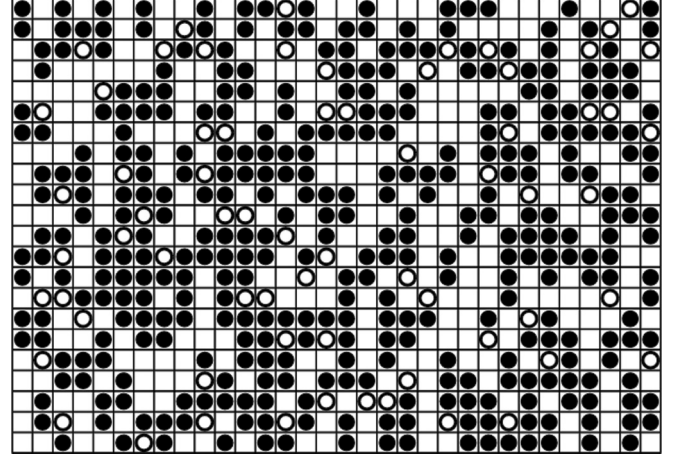


FIG. 2. Same as in Fig. 1 for model II, the nematic case,  $\theta_1 = \theta_{AB} = 0.2$  and  $\theta_2 = \theta_{AA} = 0.4$ .

To study the percolation properties of the system, the scheme described in the previous section was used. Thus,  $R_L^U(\theta_1, \theta_2)$  was calculated as a function of  $\theta_2$  for each model, each fixed value of  $\theta_1$ , and different lattice sizes ( $L = 64, 100, 128, 160, 200, 256$ , and  $320$ ). For model II (the isotropic case), the calculations were extended up to  $L = 400$ ; and for model III (the isotropic and nematic cases), the simulations were performed up to  $L = 600$ .

In Fig. 3, the variation of the percolation probability  $R_L^U(\theta_1, \theta_2)$  with  $\theta_2$  is shown for a typical case: for model I, the isotropic case,  $\theta_1 = \theta_{AA} = 0.4$  and different values of  $L$ , as indicated. As can be observed, for increasing values of  $L$ , the transition between nonpercolating and percolating regions becomes more abrupt, and the value of  $\theta_2$  ( $=\theta_2^c$ ) corresponding to the inflection point of  $R_L^U(\theta_1, \theta_2)$  [maximum in the derivative of  $R_L^U(\theta_1, \theta_2)$  with respect to  $\theta_2$ ] increases.

Figure 4 shows the extrapolation of  $\theta_2^c(L)$  toward the thermodynamic limit according to the analytical prediction given by Eq. (1) for the data in Fig. 3. Symbols represent simulation results, and the solid line is the theoretical fit from Eq. (1). This is how we obtain the percolation threshold for each model and degree of alignment, and each particular value of  $\theta_1$ .

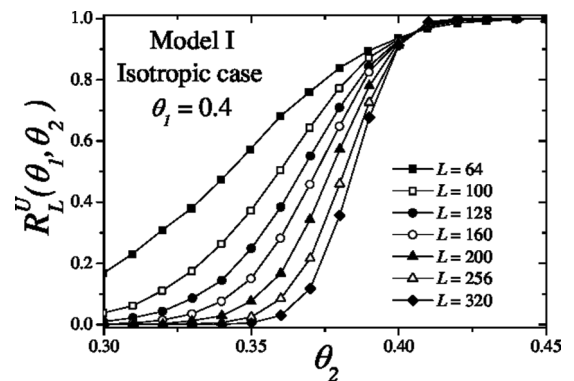


FIG. 3. Fraction of percolating lattices  $R_L^U(\theta_1, \theta_2)$  as a function of  $\theta_2$  for model I, the isotropic case, and  $\theta_1 = \theta_{AA} = 0.4$ . Different values of  $L$  are considered, as indicated.

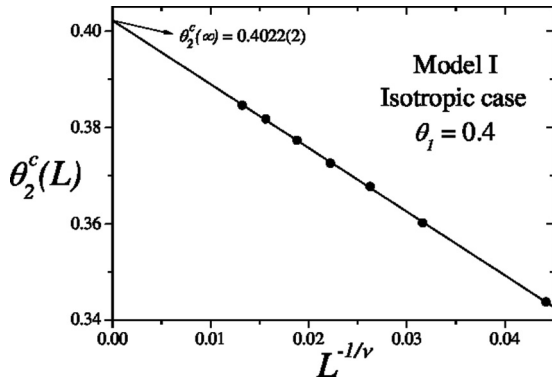


FIG. 4. Extrapolation of  $\theta_2^c(L)$  toward the thermodynamic limit according to the theoretical prediction given by Eq. (1), and the same parameters as in Fig. 3. Symbols represent simulation results, and the solid line is the theoretical fit from Eq. (1).

The study in Figs. 3 and 4 was repeated for models I–III (the isotropic case and different values of  $\theta_i$ ). The results, shown in Fig. 5, represent the complete percolation phase diagram of isotropic dimers deposited on square lattices. To better compare the three models, the data in Fig. 5 are presented in terms of  $\theta_{AA}$  (horizontal axis for models I–III),  $\theta_{AB}$  (vertical axis for models I and II), and  $\theta_{BB}$  (vertical axis for model III).

Figure 5 includes the curve of limiting values of the total coverage (solid line). This curve is obtained from the jamming conditions (i)  $\theta_{AA} + \theta_{AB} \leq \theta_j = 0.907(3)$  (models I and II) and (ii)  $\theta_{AA} + \theta_{BB} \leq \theta_j = 0.907(3)$  (model III), where  $\theta_j = 0.907(3)$  is the jamming coverage corresponding to isotropic dimers on square lattices [6]. The region below this jamming curve represents the space of all the allowed values of the total coverage ( $\theta_{AA} + \theta_{AB}$  for models I and II, and  $\theta_{AA} + \theta_{BB}$  for models III). On the other hand, the region above this curve corresponds to a forbidden region of the space of values of the total coverage.

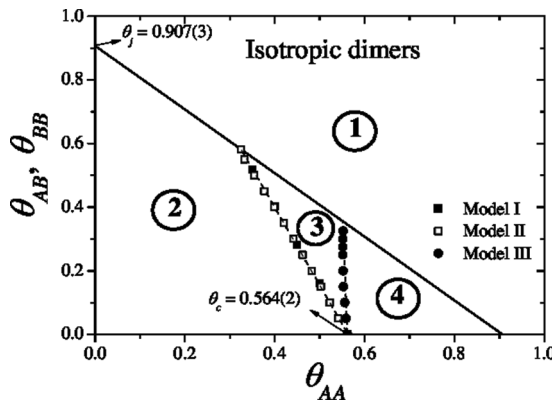


FIG. 5. Percolation phase diagram of isotropic dimers for model I (solid squares), model II (open squares), and model III (solid circles). The symbols divide percolating from nonpercolating regions for each model. Region 1: forbidden region for models I, II, and III; region 2: nonpercolating region for models I, II, and III; region 3, percolating region for models I and II, and nonpercolating region for model III; and region 4, percolating region for models I, II, and III. In all cases, the error bar is smaller than the size of the symbols.

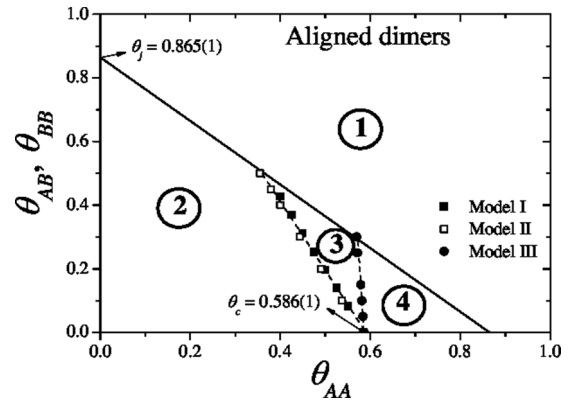


FIG. 6. Same as Fig. 5 for perfectly aligned dimers (isotropic case).

Once the allowed space of the parameters  $\theta_{AA}$ ,  $\theta_{AB}$ , and  $\theta_{BB}$  is determined, the percolation results will be analyzed in the following. For each model, the separation line between percolating and nonpercolating regions was calculated: model I (solid squares), model II (open squares), and model III (solid circles). In the case of models I and II, a perfect coincidence is observed in the separation lines. This finding indicates that the order at which the dimers are deposited does not affect the proportion of each kind that leads to percolation. In fact, the deposition scheme can be thought of as a process with two steps. The first step consists of depositing nonlabeled dimers until a coverage  $\theta_1 + \theta_2 < \theta_j$  is reached. In the second step, the dimers are randomly labeled with AA and AB, according to the desired fractions. There are different ways to perform this second step. Among them, model I (II) corresponds to the case in which AA (AB) dimers are labeled in a first stage, and AB (AA) dimers are labeled in a second stage ( $AA \rightarrow AB$ ) [ $AB \rightarrow AA$ ]. Moreover, the different types of dimers could be labeled simultaneously with adequate probabilities. Clearly, the obtained results do not depend on the order in which the dimers are labeled.

With respect to model III, and as is expected, the values of  $\theta_{AA}$  remain approximately constant around 0.564 (see the discussion in the next paragraph), and they do not depend on  $\theta_{BB}$ . The inverse of model III is trivial (see Sec. II and the previous paragraph).

As can be seen, for the three studied models the separation lines between percolating and nonpercolating regions are linear functions, and they cut the abscissa axis at the point  $\theta_{AA} = 0.564$ . This value was extrapolated by employing the already known percolating threshold of  $\theta_c = 0.564(2)$  for isotropic dimers on square lattices [38,39]. In this limit, only AA dimers are present in the system.

To summarize the results in Fig. 5, four regions were indicated in the figure. Region 1: forbidden region for models I, II, and III; region 2: nonpercolating region for models I, II, and III; region 3, percolating region for models I and II, and nonpercolating region for model III; and region 4, percolating region for models I, II, and III.

Figure 6 shows the percolation phase diagram for perfectly aligned dimers according to models I, II, and III. Symbols are as in Fig. 5. The line separating the allowed from the forbidden

region is also present, and the jamming coverage for nematic dimers on square lattices is  $\theta_j = 0.865(1)$  [45]. The behavior of the boundary lines between percolating and nonpercolating regions is qualitatively similar to that discussed in Fig. 5. In this case, the  $x$  intercept is equal to 0.586. This value corresponds to the percolation threshold for aligned dimers on square lattices,  $\theta_c = 0.586(1)$  [45].

In a recent work by Tarasevich *et al.* [17], a model of isotropic  $k$ -mers with defects was studied. The  $k$ -mers contain an average fraction  $d$  of nonconductive segments (defects). Given that  $d$  is an average fraction, a mixture of different  $k$ -mers is deposited on the lattice. In the particular case of dimers ( $k = 2$ ), three types of particles are deposited: ideal dimers (formed by two conductive segments), nonconductive dimers (formed by two nonconductive segments), and partially conductive dimers (formed by one conductive segment and one nonconductive segment). In Ref. [17], the fraction of conductive segments corresponding to percolation was calculated as a function of the fraction of defects  $d$ .

The results reported by Tarasevich *et al.* [17] can be compared with the present data for models I–III and the isotropic case. In our case, the fraction of defects can easily be calculated as

$$d = \frac{1}{2} \left( \frac{\theta_{AB}}{\theta_{AA} + \theta_{AB}} \right) \quad (\text{models I and II}) \quad (2)$$

and

$$d = \frac{\theta_{BB}}{\theta_{BB} + \theta_{AA}} \quad (\text{model III}). \quad (3)$$

In addition, the fraction of conductive segments ( $\theta_A$ ) can be calculated as

$$\theta_A = (\theta_{AA} + \theta_{AB})(1 - d) \quad (\text{models I and II}) \quad (4)$$

and

$$\theta_A = (\theta_{AA} + \theta_{BB})(1 - d) \quad (\text{model III}). \quad (5)$$

Figure 7 shows the fraction of conductive segments corresponding to percolation ( $\theta_A^c$ ) as a function of the fraction of defects for dimers deposited on square lattices according to model I (solid squares), model II (open squares), model III (solid circles), and the model proposed in Ref. [17] (open circles). The solid lines are simply a guide for the eye.

For model III, percolation occurs only through conductive  $AA$  dimers, and, as in the classical problem of dimers on square lattices [38,39],  $\theta_A^c(d)$  remains practically constant around 0.56. On the other hand, in the case of models I and II,  $AA$  and  $AB$  dimers are part of the percolating cluster. As in previous work [17], the presence of defective  $AB$  dimers produces the observed increase in  $\theta_A^c(d)$ .

It can be seen that the data from Ref. [17], which correspond to the case in which three types of dimers are mixed ( $AA$ ,  $BB$ , and  $AB$ ), fall in an intermediate region between our two limit cases: the case corresponding to a mixture of  $AA$  and  $AB$  dimers (models I and II), and the case corresponding to a mixture of  $AA$  and  $BB$  dimers (model III). The analysis in

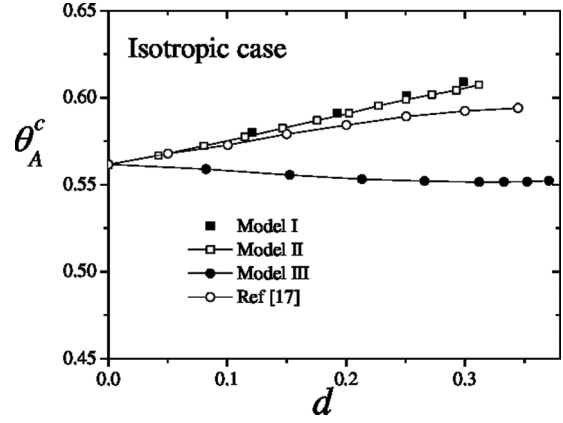


FIG. 7. Fraction of conductive segments corresponding to percolation ( $\theta_A^c$ ) as a function of the fraction of defects ( $d$ ) for dimers deposited on square lattices according to model I (solid squares), model II (open squares), model III (solid circles), and the model proposed in Ref. [17] (open circles). The solid lines are simply a guide for the eye. In all cases, the error bar is smaller than the size of the symbols.

Fig. 7 show that our results are consistent with the previous ones obtained by Tarasevich *et al.* [17].

#### IV. CONCLUSIONS

Irreversible deposition of dimers on a square homogeneous lattice was studied. The presence of defects in the dimers was analyzed. This was introduced as two kinds of segments composing the dimers: type  $A$  (percolating) and type  $B$  (non-percolating). Three different models were considered. Model I consisted in depositing  $AA$  dimers in a first stage and  $AB$  dimers in a second stage. Model II consisted in depositing  $AB$  dimers in a first stage and  $AA$  dimers in a second stage. Finally, model III consisted in depositing  $BB$  dimers in a first stage and  $AA$  dimers in a second stage. The connectivity analysis was carried out by accounting only for the conductive segments.

On the other hand, two ways of deposition were taken into account: isotropic (with equal probability in both directions) or nematic (with all the dimers aligned in one direction). The percolation threshold was analyzed for each model and deposition mechanism. A linear behavior was reported for the relationship between the coverage degree of the two species in the percolation phase diagram. The present results were found to be consistent with those from a previous work of Tarasevich *et al.* in the context of deposition of defective  $k$ -mers [17].

#### ACKNOWLEDGMENTS

This work was supported in part by CONICET (Argentina) under Project No. PIP 112-201101-00615; Universidad Nacional de San Luis (Argentina) under Project No. 322000; and the National Agency of Scientific and Technological Promotion (Argentina) under Project No. PICT-2013-1678. The numerical work was done using the BACO parallel cluster (composed of 50 PCs each with an Intel i7-3370/2600 processor) located at Instituto de Física Aplicada, Universidad Nacional de San Luis–CONICET, San Luis, Argentina.

- [1] L. Onsager, *Ann. NY Acad. Sci.* **51**, 627 (1949).
- [2] A. Stroobants, H. N. W. Lekkerkerker, and Th. Odijk, *Macromolecules* **19**, 2232 (1986).
- [3] A. Ghosh and D. Dhar, *Europhys. Lett.* **78**, 20003 (2007).
- [4] J. Kundu, R. Rajesh, D. Dhar, and J. F. Stilck, *Phys. Rev. E* **87**, 032103 (2013).
- [5] J. Kundu and R. Rajesh, *Phys. Rev. E* **89**, 052124 (2014).
- [6] J. W. Evans, *Rev. Mod. Phys.* **65**, 1281 (1993).
- [7] V. Privman, *Colloids Surf. A* **165**, 231 (2000).
- [8] J. Talbot, G. Tarjus, P. R. Van Tassel, and P. Viot, *Colloids Surf. A* **165**, 287 (2000).
- [9] J. Feder, *J. Theor. Biol.* **87**, 237 (1980).
- [10] P. L. Krapivsky, S. Redner, and E. Ben-Naim, *A Kinetic View of Statistical Physics* (Cambridge University Press, Cambridge, UK, 2010).
- [11] B. Bonnier, M. Hontebeyrie, Y. Leroyer, C. Meyers, and E. Pommiers, *Phys. Rev. E* **49**, 305 (1994).
- [12] N. Vandewalle, S. Galam, and M. Kramer, *Eur. Phys. J. B* **14**, 407 (2000).
- [13] G. Kondrat and A. Pękaliski, *Phys. Rev. E* **63**, 051108 (2001).
- [14] N. I. Lebovka, N. N. Karmazina, Y. Y. Tarasevich, and V. V. Laptev, *Phys. Rev. E* **84**, 061603 (2011).
- [15] Y. Yu. Tarasevich, N. I. Lebovka, and V. V. Laptev, *Phys. Rev. E* **86**, 061116 (2012).
- [16] N. I. Lebovka, Y. Yu. Tarasevich, D. O. Dubinin, V. V. Laptev, and N. V. Vygornitskii, *Phys. Rev. E* **92**, 062116 (2015).
- [17] Y. Yu. Tarasevich, V. V. Laptev, N. V. Vygornitskii, and N. I. Lebovka, *Phys. Rev. E* **91**, 012109 (2015).
- [18] Y. Yu. Tarasevich, A. S. Burmistrov, T. S. Shinyaeva, V. V. Laptev, N. V. Vygornitskii, and N. I. Lebovka, *Phys. Rev. E* **92**, 062142 (2015).
- [19] H. Harder, A. Bunde, and W. Dieterich, *J. Chem. Phys.* **85**, 4123 (1986).
- [20] H. Holloway, *Phys. Rev. B* **37**, 874 (1988).
- [21] Z. Gao and Z. R. Yang, *Physica A* **255**, 242 (1998).
- [22] M. Dolz, F. Nieto, and A. J. Ramirez-Pastor, *Eur. Phys. J. B* **43**, 363 (2005).
- [23] Y. Y. Tarasevich and V. A. Cherkasova, *Eur. Phys. J. B* **60**, 97 (2007).
- [24] V. A. Cherkasova, Y. Y. Tarasevich, N. I. Lebovka, and N. V. Vygornitskii, *Eur. Phys. J. B* **74**, 205 (2010).
- [25] W. Lebrecht, J. F. Valdés, E. E. Vogel, F. Nieto, and A. J. Ramirez-Pastor, *Physica A* **392**, 149 (2013).
- [26] M. I. González, P. M. Centres, W. Lebrecht, A. J. Ramirez-Pastor, and F. Nieto, *Physica A* **392**, 6330 (2013).
- [27] W. Lebrecht, J. F. Valdés, E. E. Vogel, F. Nieto, and A. J. Ramirez-Pastor, *Physica A* **398**, 234 (2014).
- [28] M. C. Gimenez and A. J. Ramirez-Pastor, *Physica A* **421**, 261 (2015).
- [29] J. M. Hammersley, *Proc. Cambridge Philos. Soc.* **53**, 642 (1957).
- [30] J. W. Essam, *Rep. Prog. Phys.* **43**, 833 (1980).
- [31] R. Zallen, *The Physics of Amorphous Solids* (Wiley, New York, 1983).
- [32] *Percolation Structures and Processes*, Annals of the Israel Physical Society Vol. 5, edited by G. Deutscher, R. Zallen, and J. Adler (Hilger, Bristol, 1983).
- [33] M. Sahimi, *Applications of Percolation Theory* (Taylor & Francis, London, 1994).
- [34] D. Stauffer and A. Aharony, *Introduction to Percolation Theory* (Taylor & Francis, London, 1994).
- [35] G. Grimmett, *Percolation* (Springer-Verlag, Berlin, 1999).
- [36] B. Bollobás and O. Riordan, *Percolation* (Cambridge University Press, New York, 2006).
- [37] This value represents the jamming coverage corresponding to dimers on square lattices [6].
- [38] V. Cornette, A. J. Ramirez-Pastor, and F. Nieto, *Physica A* **327**, 71 (2003).
- [39] V. Cornette, A. J. Ramirez-Pastor, and F. Nieto, *Eur. Phys. J. B* **36**, 391 (2003).
- [40] K. Binder, *Rep. Prog. Phys.* **60**, 487 (1997).
- [41] F. Yonezawa, S. Sakamoto, and M. Hori, *Phys. Rev. B* **40**, 636 (1989).
- [42] F. Yonezawa, S. Sakamoto, and M. Hori, *Phys. Rev. B* **40**, 650 (1989).
- [43] J. Hoshen and R. Kopelman, *Phys. Rev. B* **14**, 3438 (1976).
- [44] M. C. Gimenez, F. Nieto, and A. J. Ramirez-Pastor, *J. Phys. A* **38**, 3253 (2005).
- [45] P. Longone, P. M. Centres, and A. J. Ramirez-Pastor, *Phys. Rev. E* **85**, 011108 (2012).